Journal of
Mechanical
Science and
Technology

Journal of Mechanical Science and Technology 21 (2007) 2205~2213

Analysis of diesel spray structure using a hybrid model

Sungsik Chung, Jongsang Park, Sipom Kim and Jeongkuk Yeom*

Division of Mechanical Engineering, Dong-A University, Busan 604-714, Korea

(Manuscript Received August 23, 2006; Revised October 25, 2007; Accepted October 28, 2007)

Abstract

This study proposes a hybrid model that consists of modified Taylor Analogy Breakup (TAB) model and a Discrete Vortex Method (DVM). In this study the simulation is divided into three steps. The first step is to analyze the breakup of the injected fuel droplets by using a modified TAB model. The second step is based on Siebers' theory of liquid length, which is an analysis of spray evaporation. The liquid length analysis for injected fuel is used to connect both the modified TAB model and the DVM. The final step is to reproduce the ambient gas flow and the inner vortex flow of the injected fuel by using the DVM. In order to examine this hybrid model, we performed an experiment involving a free evaporating fuel spray at the early injection stage within an environment similar to that found inside of an engine cylinder. The numerical results were calculated by using the present hybrid model and compared to the experimental results. The calculated results of the gas jet flow that were determined through the DVM corresponded well with the experimental results for a downstream evaporative spray. It is also confirmed that an ambient gas flow occupies the downstream region of a diesel spray.

Keywords: Exciplex fluorescence method; Modified TAB model; DVM (Discrete Vortex Method); Liquid length; Evaporative spray; Vortex

1. Introduction

There have been a variety of simple models with various CFD in the field of spray analysis and spray combustion, a few such studies include: KIVA (KIVA-II, KIVA-3, and KIVA-3V) [1-4] proposed by Los Alamos Lab., and STAR-CD [5]. We have built a model that can describe the breakup and diffusion process of a diesel impinging and free spray [6-8]. However, it was discovered that these models could not precisely express the micro-characteristics of an injected spray, such as spray tip penetration, nor the inner structure of a diesel spray. Therefore, in order to reliably predict the inner-structure and micro-characteristics of a diesel spray, this study proposes a hybrid model that consists of a modified TAB model [9] and a DVM [10]. In this study, the simulation is divided into three steps. The first step is to analyze the breakup of the injected fuel droplets by using a KIVA-II TAB model. The second step is based on Siebers' liquid length theory of spray evaporation and switching both the TAB model and the DVM. The final step is to reproduce the ambient gas flow and the inner vortex of the injected fuel by using the DVM. The schematic concept of this hybrid model is shown in Fig. 1.

There have been previous spray structure studies conducted using a DVM [11, 12]; however, these studies neglected the liquid phase of the injected spray by only applying the DVM to the end point of the injected fuel evaporation. Furthermore, these studies only dealt with the flow of the vapor phase of the injected fuel and ambient gas. Therefore, this study analyzes the flow of the liquid phase before the end of the injected fuel evaporation by introducing the liquid phase length based on the concept by Siebers. We found that the results of the hybrid model, which included the improved TAB model and DVM, were all in good agreement with the experimental results.

*Corresponding author. Tel.: +82 51 200 7640, Fax.: +82 51 200 7656
E-mail address: laser355@dau.ac.kr

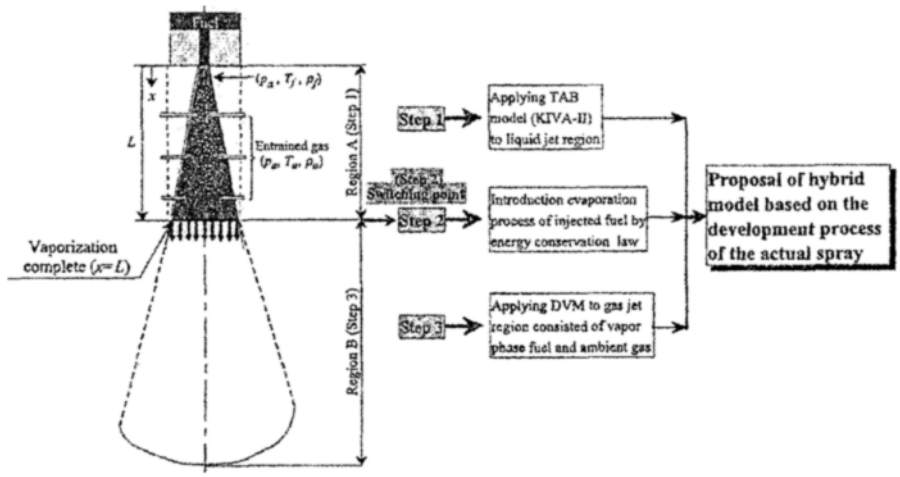

Fig. 1. Hypothesized spray structure with two-regions for simulation.

Table 1. Experimental Conditions.

Injection nozzle	Type : Hole nozzle DLL-p	
	Diameter of hole d_n [mm]	0.2
	Length of hole L_n [mm]	1.0
Ambient gas		N_2 gas
Ambient temperature	T_a [K]	700
Ambient pressure	P_a [MPa]	2.55
Ambient density	ρ_a [kg/m^3]	12.3
Injection pressure	P_{inj} [MPa]	72
Injection quantity	Q_{inj}[mg]	12.0
Injection duration	t_{inj} [ms]	1.54

2. Experimental and simulation conditions

2.1 Experimental conditions

The n-tridecane that was used as the reference fuel oil for the JIS second class gas oil was injected into a quiescent atmosphere of nitrogen gas through a single hole injector. A 9% mass of naphthalene and 1% of TMPD (N,N,N',N' tetramethyl-p-phenylene diamine) were mixed with n-tridecane to obtain the fluorescent emissions of the vapor and liquid phases. The TMPD was mixed with n-tridecane in a nitrogen atmosphere to prevent the oxidation of the TMPD. A high pressure injection system (ECD-U2 system) developed by Denso Co., Ltd. was used in this experiment. The diameter and the length of nozzle were 0.2 mm and 1.0 mm, respectively. A summary of the experimental conditions can be found in Table 1.

Fig. 2 shows a schematic of the optical system used in this study. The light source was the third harmonic of an Nd:YAG laser at 355 nm (power: 60 mJ/pulse, pulse width: 8 nsec., maximum frequency: 10 Hz, beam diameter: 6.4 mm, beam shape: doughnut type).

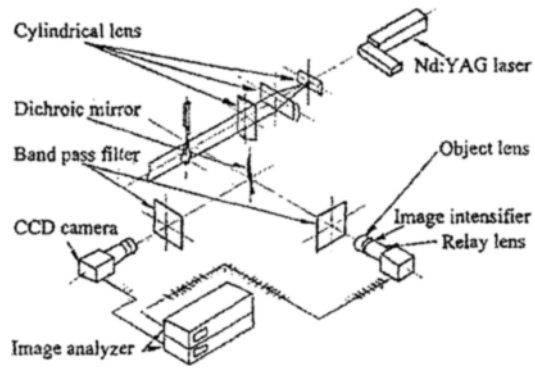

Fig. 2. Schematic diagram of laser sheet optical system and photography system.

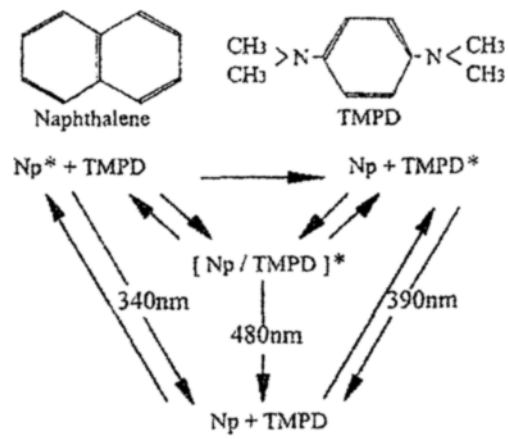

Fig. 3. Schematic summary of naphthalene and TMPD exciplex system.

Fig. 3 shows, a schematic summary of the photophysics of the naphthalene and TMPD exciplex fluorescence system proposed by Melton et al. [13].

Table 2. Computational Conditions (for KIVA-II code).

Injection velocity V_{inj} [m/s]	338
Injection duration t_{inj} [ms]	1.54
Injection quantity Q_{inj} [mg]	12.0
Initial droplet temperature T_{inj} [K]	293
Fuel	n-Tridecane
Number of parcel N_p	1000
Ambient temperature T_a [K]	700
Ambient density ρ_a [kg/m^3]	12.3
Maximum time step dt_{max} [s]	1.0×10^{-6}
Minimum time step dt_{min} [s]	0.5×10^{-8}
Number of mesh	23×1×70 (sector mesh)

2.2 Simulation conditions

2.2.1 Improved KIVA-II code

Table 2 shows the calculation condition of the KIVA-II method used in this study. The values of the calculation conditions correspond with the experimental conditions mentioned above.

2.2.2 DVM model

DVM based on Lagrangian analysis is a flow analysis method for the motion of each free vortex, which replaces the continued distribution of vorticity, that occurs in a flow having different viscosity and density with discrete distribution of free vortex. Previous studies applied the DVM method, which was first proposed by Rosenhead [14], mainly to separation flow and gas jet with a comparatively high Reynolds number [15]. The DVM is simple to implement and effective in modeling the essence of vortex formation, and fit for coupling with the model of interaction between particles and fluid because both drop-phase and gas-phase are solved in Lagrangian form. By using DVM, this study deals with the gas jet flow of 2-dimensional unsteady based on the assumption of incompressible fluid. In the DVM, the representative models of viscosity considered are the Random Walk Method [16] and vortex core model [17]. The vortex core model was used in this study. In the case of an inviscid vortex, vorticity diffusion is not occurring; however, in the case of a viscosity vortex, the temporal diffusion of vorticity should be considered.

Fig. 4 shows the coordinate system for DVM calculation.

As for the solution of the 2-dimensional Navier-Stokes equation in the viscosity vortex, vorticity distribution of time T and radius r_v from center can be obtained by the following equation (Nagano [17]).

$$\omega(r_v,T)=\frac{\Gamma}{4\pi\nu t}\exp\left(-\frac{r_v\mathrm{Re}}{4T}\right) \tag{1}$$

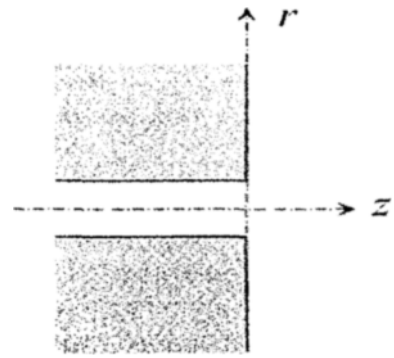

Fig. 4. Coordinate system of flow field for DVM.

Where ω is vorticity, which is circulation of discrete vortex, and r_v is the radial distance from the vortex center, respectively. Also, in the case of considering vorticity diffusion, the induced velocity can be expressed as the following equation:

$$\begin{aligned} u(T)&=\frac{\Gamma(r_0-r)}{2\pi R^2}\left\{1-\exp\left(-\frac{r_v^2\mathrm{Re}}{4T}\right)\right\}\\ v(T)&=-\frac{\Gamma(z_0-z)}{2\pi R^2}\left\{1-\exp\left(-\frac{r_v^2\mathrm{Re}}{4T}\right)\right\}\end{aligned} \tag{2}$$

Where u is the velocity component in z-axis direction, and v is the velocity component in r-axis direction. Each velocity $u(T)$ and $v(T)$ is equal to 0 at the vortex center. With increasing radius r_v, the velocities also increase and become maximum value at a position σ'. The position σ' increases with time. The case where the vortex is concentrated on one point at T=0 can be explained by the following equation.

$$\sigma'=2.242(T/\mathrm{Re})^{0.5} \tag{3}$$

In Eq. (3), assuming that σ' is vortex core radius and vorticity is constant in the vortex core, Eqs. (1) and (2) can be expressed by eqs (4) and (5) below:

$$\omega=\begin{cases}\dfrac{\Gamma}{\pi\sigma'} & (r_v\le\sigma')\\ 0 & (r_v>\sigma')\end{cases} \tag{4}$$

$$\begin{aligned} u&=\frac{\Gamma(r_0-r)}{2\pi\sigma'^2},\ v=-\frac{\Gamma(z_0-z)}{2\pi\sigma'^2} \quad (r_v\le\sigma')\\ u&=\frac{\Gamma(r_0-r)}{2\pi R^2},\ v=-\frac{\Gamma(z_0-z)}{2\pi R^2} \quad (r_v>\sigma')\end{aligned} \tag{5}$$

2.2.3 Analysis of liquid phase length for switching both the TAB model and DVM model

In order to investigate the liquid phase length, three non-dimensional groups were used from Siebers' analysis [18] of liquid-phase length. These groups correspond to a momentum scale, an energy scale, and a length scale. From a consideration of the conservation of mass and momentum, the liquid phase length should have a function dependence on the ratio of the fuel density (ρ_f) to the in-cylinder gas density (ρ_a). In this study, the non-dimensional constant A, which can be expressed as Eq. (6), is equal to 26.4 by using the Thermophysical Properties of Hydrocarbon Mixture Database (i.e., "NIST program"), [19].

$$A = \frac{\rho_f}{\rho_a} \tag{6}$$

Also, the heat transfer from the ambient gas to injected fuel is considered, and the parameter is denoted the "specific energy ratio" and is defined as follows:

$$B = \frac{C_{p,liq}\left(T_b - T_f\right) + h_{vap}}{C_{p,air}\left(T_{air} - T_b\right)} \tag{7}$$

In the above equation, the fuel properties are as follows: C_p, the specific heat at constant pressure; T_b, the boiling point temperature; T_f, the initial temperature; and h_{vap}, the latent heat of vaporization. T_a is the temperature of the in-cylinder gases. Also, according to Ely et al. [19], in this study, the value of $C_{p,liq}$ and $C_{p,air}$ is, respectively, 4.48 and 1.11 kJ/kgK. The value of h_{vap} is determined by using an estimation method [20] and equal to 57.53 kJ/kg, here. Finally, a length scale for fuel properties from the results of Siebers et al. [18] can be expressed:

$$\ln\left(\frac{x_{liq}}{d_0}\right) = \ln k' + \alpha \ln A + \beta \ln B \tag{8}$$

where according to the results of Siebers et al. [18], the k', α, and β are constants whose value are, 10.5, 0.58, and 0.59, respectively. Using this equation, the liquid length x_{liq} calculated to 36 mm for the experimental condition of this study.

The calculation condition of DVM is the same as that of KIVA-II code. As the object of DVM is turbulent gas jet, the simulated DVM needs to set a gas velocity U_0 m/s, the diameter of gas jet H mm, and kinematic viscosity of ambient gas ν_g mm^2/s as the initial conditions. Thus those parameters are obtained by Dan et al. [8] based on the conservation of the momentum equal to the diesel spray. The mechanism of the DVM is related to the concept of the diffusion process of droplets by Kosaka et al. [12]. The momentum between the diesel spray and the gas jet is related as follows.

$$\mathrm{H} \cdot \mathrm{U}_0 = \left(\rho_l / \rho_g\right)^{1/2} \cdot \mathrm{d}_n \cdot \mathrm{u}_{inj} \tag{9}$$

Where ρ_l is the liquid density, d_n is the nozzle hole diameter, u_{inj} is the injection velocity of liquid at the nozzle and ρ_g is the gas density. Here, the evaporated gas consists of nitrogen of ambient gas and n-tridecane of used fuel (mole fraction N_2:$C_{13}H_{28}$= 0.96:0.04) in the middle region of Z=35~65 mm from the nozzle exit. The mole fraction can be calculated by the mean fluorescence intensity and quantification scheme of vapor-phase concentration from experimental results of the exciplex fluorescence method. The density (ρ_g) of gas having such a mole fraction is 14.5 kg/m^3 in T_a=700 K and p_a=2.55 MPa by using the NIST program. Furthermore, the equivalent diameter of gas jet, H=11 mm is the spreading of vapor phase at a distance from the nozzle tip, Z=38 mm by the concept of Siebers et al. [18] and our experimental results, and H=11 mm is used in initial condition of DVM simulation. Hence, the Eq.(19) can be calculated by determining an unknown, U_0. However, in the case of U_0 calculation, H is 6.8 mm, which is the value of the spreading of liquid phase at Z=38 mm, because the liquid phase dominates the spray development in axial direction. H=6.8 mm is only used in the case of the calculation of U_0. As a result, the gas jet velocity is determined as U_0=64.2 m/s by using H=6.8 mm, and it can also be supposed that the gas jet is injected with a velocity U_0=64.2 m/s from nozzle diameter, H=11 mm. The kinematic viscosity of ambient gas ν_g is equal to 1.99 mm^2/s by the NIST program.

Table 3 shows a summary of the calculation conditions for DVM. For the calculating, non-dimensional time T is employed, and the time T is derived by $t(U_0/H)$. The time step ΔT corresponding to the time interval of vortex shedding is equal to 0.025.

Table 3. Computational Conditions. (for Discrete Vortex Method)

Nozzle hole diameter	H [mm]	11
Issue velocity	U_0 [m/s]	64.2
Gas (mole fraction)		n-Tridecane (0.04), N2 (0.96)
Gas density	ρ_g [kg/m^3]	14.5
Gas kinematic viscosity	ν_g [mm^2/s]	1.99
Reynolds number at nozzle		355000
Injection duration	T	10.0 (≈1.71[ms])
Time step	ΔT	0.025

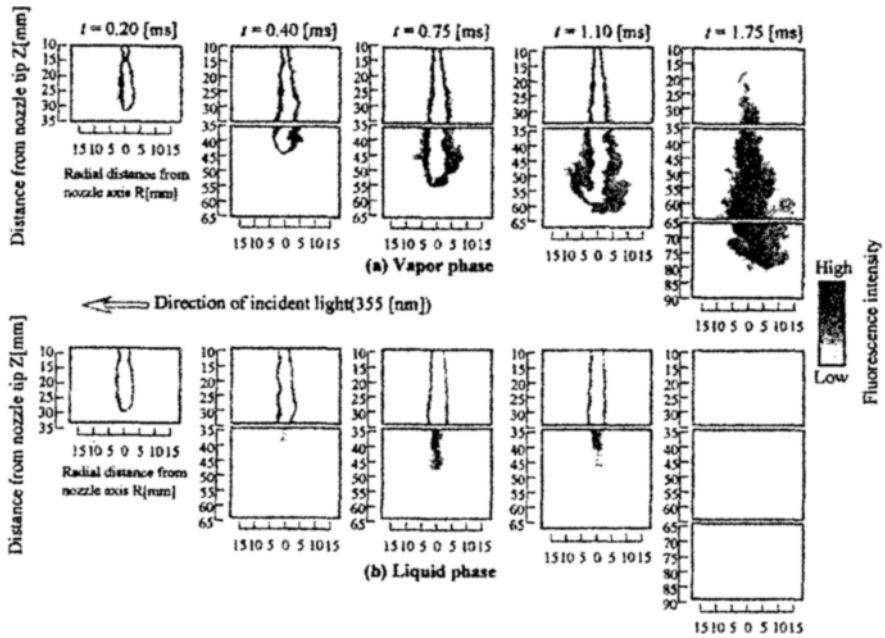

Fig. 5. Temporal change in the free spray taken by exciplex fluorescence method.
(p_{inj}=72[MPa], Q_{inj}=12.0[mg], ρ_a=12.3[kg/m^3], T_a=700[K])

3. Results and discussion

3.1 Experimental results for the exciplex fluorescence method

Fig. 5 shows the 2-dimensional fluorescence intensity images for the free spray captured by the exciplex fluorescence method. Near the central spray axis, the fluorescence intensity phenomenon exceeds the sensitivity of the CCD camera, because of the liquid phase in the vicinity of nozzle. Figs. 5(a) and (b) show the vapor and liquid phase of the injected fuel, respectively. With elapsed time, the spray tip penetration of both vapor and liquid phases increases. In Fig. 5, the image area of the liquid phase gradually decreases; however, the image area of the vapor phase increases, due to the phase change of the injected fuel. In the later stage of the injection time, the spreading of the vapor phase becomes larger due to the effect of the ambient gas. A measurement of the ambient gas flow; however, is almost impossible with the exciplex fluorescence method.

In Fig. 6 the measured tip penetration of the liquid and vapor phases is plotted against time. The horizontal axis is the non-dimensional time that represents the time from the start of the injection divided by injection duration. In this figure the liquid phase length (l_{liq}) is determined by the overall intensity region in the liquid phase image. As shown in Fig. 6, the tip penetration of the liquid and vapor phases increases with elapsed time. A value convergence of the liquid phase length could not be observed as it could in other experiments of evaporating spray [21-25].

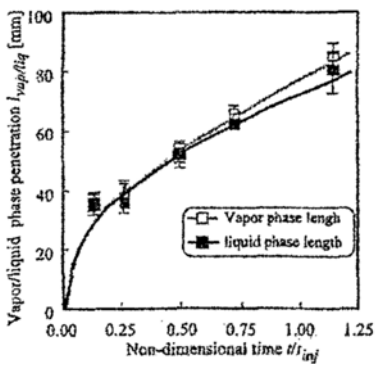

Fig. 6. Temporal change in penetrations of the vapor and liquid phase. (p_{inj}=72[MPa], Q_{inj}=12.0[mg], ρ_a=12.3[kg/m^3], T_a=700[K])

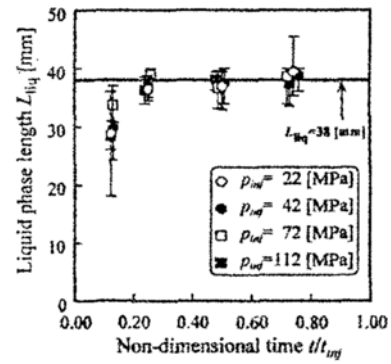

Fig. 7. Temporal change in liquid phase length.

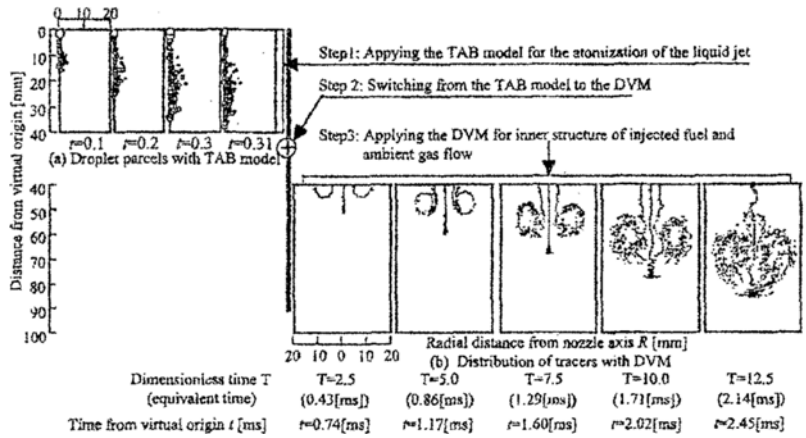

Fig. 8. Temporal change in droplet parcels with TAB model and distribution of tracers taken by DVM. (H=11 [mm], U_0=64.2 [m/s], ν_a=1.99×10^{-6} [m^2/s], Re=3.55×10^5, T_{inj}=10.0 (1.71 [ms]))

Fig. 7 shows the liquid phase length L_{liq} versus the non-dimensional time. The liquid phase length (L_{liq}) is defined by the spatial region where the fluorescence intensity ranges from 255 gradations in the spray's center to 10~20 [%] (230~255) gradations in each image. As shown in Fig. 7, the value of the liquid phase length irrespective of injection pressure is almost 38 mm in the curve. Furthermore, it was found that the tendency of the liquid phase change agrees with the start point of the spray development in the radial direction as shown in Fig. 5. Specifically, the value of 38 mm from nozzle exit corresponds to the length of the end of the momentum exchange from the liquid jet to the ambient gas [8].

3.2 Simulation results for the hybrid model with improved TAB and DVM

Fig. 8 shows the temporal change in the droplet parcels with the TAB model and the distribution of tracers with DVM (hybrid model). In this figure, the distance from the virtual origin can be used for the measurement of the real distance from nozzle exit. The time from the virtual origin (t ms) is the real time after the start of injection. As shown in Fig. 8, the origin of the DVM results locates the distance from the virtual origin to be 40 mm where the spray of the liquid jet changes into the gas jet. In the hybrid model, the spatial distance and time for switching from the TAB to the DVM are, respectively, 40 mm and 0.31ms based on the concept of Siebers and the experimental results of the exciplex fluorescence method. In Fig. 8 the separated crosswise tracers form two small vortices at T=2.5 (T is the non-dimensional time, $t\cdot(U/H)$), with elapsed time the tracers proceed downstream at T=5.0. The tracers that proceed on the central axis stagnate due to the drag force from the ambient gas. After the vortex shedding is complete, a meandering profile near the nozzle can be

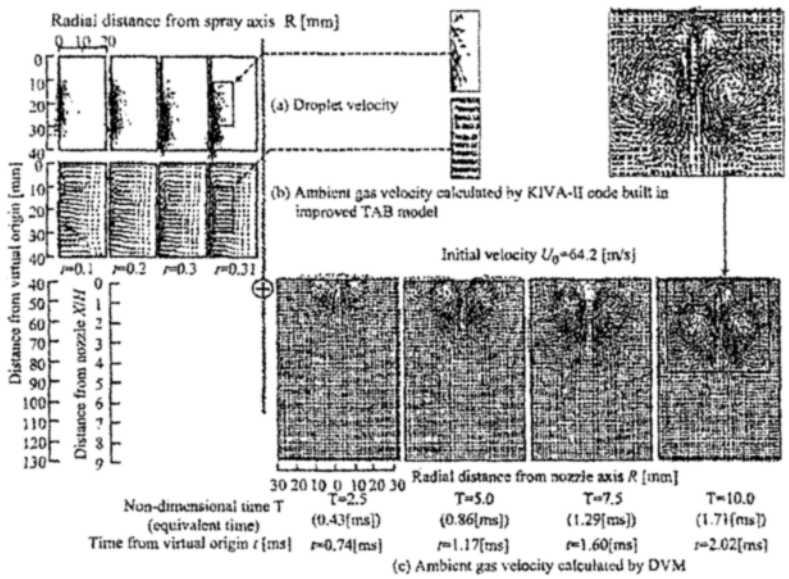

Fig. 9. Temporal change in droplet velocity and ambient gas velocity with TAB model and ambient gas velocity taken by DVM. (H=11 [mm], U_0=64.2 [m/s], ν_a=1.99×10^{-6} [m^2/s], Re=3.55×10^5, T_{inj}=10.0 (1.71 [ms]))

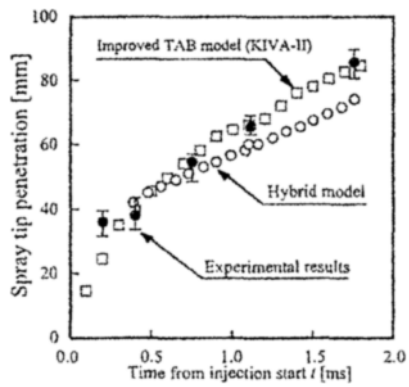

Fig. 10. Computational and experimental results for temporal change in spray tip penetration.

found. The characteristic tendency of the spray structure corresponds, qualitatively, to the experimental results.

Fig. 9 shows the temporal change in droplet velocity and ambient gas velocity with the TAB model and the ambient gas velocity by using the DVM. As shown in Fig. 9(b), although a slight flow of ambient gas occurs in the spray periphery, the entrainment phenomenon of the ambient gas cannot be seen in the inner region of the spray. Also, the vectors in the inner region of the spray proceed downstream. Hence, it was concluded that there was no entrainment of ambient gas in the liquid phase length of the injected fuel, and the momentum exchange of both the injected fuel and the ambient gas mainly occurred at the liquid phase length region of the diesel spray. On the other hand, in Fig. 9(c) [the region of DVM beyond 40 mm from the nozzle exit (Step 3)], the vectors of the ambient gas are rotating in the region of the inner spray due to the momentum exchange in the upper region of the spray; specifically, the entrainment of ambient gas takes place from the region that is the maximum penetration distance of the liquid phase fuel at 40 mm. As a result, it can be assumed that the results from the hybrid model sufficiently explain the development process and structural characteristics of a diesel spray in an evaporating field just as [26] related to a non-evaporating fuel spray. Furthermore, it can be found that the velocity distribution at each time shows a circulation flow profile separated crosswise at the region of the spray's tip. The circulations proceed downstream of the gas jet and the scale of circulation flow gradually becomes larger with elapsed time. This figure, like the case of tracer distribution, also shows the profile of the meandering flow at the end of injection.

Fig. 10 shows results of penetration for the result of the experiment, improved TAB model, and hybrid model. The spray tip penetration in the experiment and improved TAB model are the measurement results for the vapor phase of the fuel, respectively. In the figure, the simulation method of the improved TAB and hybrid model can successfully predict the

spray tip penetration under the condition of evaporating diesel fuel spray. However, with the improved TAB model, the structure of the inner spray and ambient gas flow could not be precisely reproduced. Therefore, the hybrid model proposed in this study is useful to model diesel fuel sprays, properly accounting for the characteristics of spray structure and ambient gas flow.

4. Conclusions

In this study an experiment and simulation were performed for an evaporating fuel spray. In the experiment the exciplex fluorescence method was used, which can simultaneously measure the vapor and liquid phase of injected fuel. The simulation was performed by using a hybrid model consisting of a TAB model and a vortex method

The following conclusions are drawn from this study.

(1) Applying the improved TAB model with Φ (degree of freedom)=6 and K (energy ratio of particle motion)=0.89 to the evaporating fuel spray is sufficiently useful for analyzing the spray structure, such as the spray tip penetration of the liquid and vapor phase.

(2) The hybrid model used in this study can analyze not only flow of injected fuel, but also the flow of ambient gas in the evaporative fuel spray.

(3) In the results of the hybrid model, the calculations using the DVM that were related to the gas flow correspond quantitatively to the experimental results downstream of the evaporative spray. It is also confirmed that ambient gas flow occupies the flow of the downstream region in a diesel spray.

(4) A hybrid model consisting of an improved TAB model and a DVM can properly reproduce the structural characteristics of a diesel spray in an evaporating field undergoing phase change.

Acknowledgments

This Paper was Supported by Dong-A University Research Fund in 2005.

Nomenclature

d : Diameter
H : Diameter of Gas Jet
T : Non-dimensional Time
U : Gas Velocity
u : Injection Velocity of Liquid at the Nozzle

Greek symbols

ν : Kinematic Viscosity of Ambient Gas
ρ : Density

Subscripts

g : Ambient Gas
inj : Injection
n : Nozzle
liq : Liquid Phase
vap : Vapor Phase

References

[1] A. A. Amsden, KIVA-3 : A KIVA Program with block-structured mesh for complex geometries, Los Alamos National Laboratory report LA-12503-MS, (1993).

[2] A. A. Amsden, KIVA-3V : A block-structured KIVA program for engines with vertical or canted valves, Los Alamos National Laboratory report LA-13313-MS, (1997).

[3] A. A. Amsden, P. J. O'Rourke and T. D. Butler, KIVA-II : A computer program for chemically reactive flows and sprays, Los Alamos National Laboratory report LA-11560-MS, (1989).

[4] A. A. Amsden, J. D. Ramshow, P. J. O'Rourke and J. K. Dukowiez, KIVA : A computer program for two- and three-dimensional fluid flows with chemical reactions and fuel sprays, Los Alamos National Laboratory report LA-10254-MS, (1985).

[5] B. Ahmadi-Befrui, N. Uchil, A. D. Gosman and R. Issa, Modeling and simulation of thin liquid films formed by spray-wall interaction, SAE Paper, No. 960627, (1996).

[6] J. Senda, M. Kobayashi, S. Iwashita and H. Fujimoto, Modeling of diesel spray impinging on a flat wall, SAE Paper, No. 941894, (1994).

[7] J. Senda, T. Dan, S. Takagishi, T. Kanda and H. Fujimoto, Spray characteristics of non-reacting diesel fuel spray by experiments and simulations with KIVA II code, Proceedings of ICLASS-'97(in Seoul) (1997) 38-45.

[8] T. Dan, S. Takagishi, J. Senda and H. Fujimoto, Organized structure and motion in diesel spray, *SAE Paper*, No. 970641, (1997).

[9] P. J. O'Rourke and A. A. Amsden, The TAB method for bumerical calculation of spray drop breakup, *SAE Paper*, No. 872089, (1987).

[10] Y. Yamane, T. Kamimoto, H. Kosaka and H. Kobayashi, Numerical simulation of entrainment of an

unsteady 2-D turbulent jet, *Transaction of JSME(in Japanese) B*. 60 (572) (1994) 1457-1462.

[11] T. Kamimoto, Y. Yamane, H. Kosaka and H. Kobayashi, Numerical simulation of turbulent mixing in a transient jet, SAE Paper, No. 932657, (1993).

[12] H. Kosaka, T. Suzuki and T. Kamimoto, Numerical simulation of turbulent dispersion of fuel droplets in an unsteady spray via discrete vortex method, SAE Paper, No. 952433, (1995).

[13] L. A. Melton, Spectrally separated fluorescence emissions for diesel fuel droplets and vapor, Applied Optics, 22 (1) (1983) 2224-2226.

[14] L. Rosenhead, The formation of vortices from a surface of discontinuity, Proc. R. Soc. Lond. A-134 (1931)170-192.

[15] S. Shimizu, An analysis of a two-dimensional jet by the discrete Vortex simulation, *Transactions of JSME* B. 472 (1985) 3852-3859.

[16] A. J. Chorin, Numerical study of slightly viscous flow, *J. Fluid Mech.* 57 (4) (1973) 785-796.

[17] H. Sakata, T. Adachi and T. Inamuro, A Numerical analysis of unsteady separated flow by discrete vortex model (1st report, flow around a square prism), *Transactions of JSME B*(in Japanese). 49 440 (1983) 801-808.

[18] D. L. Siebers, J. Charles and B. S. Higgins, Measurements of fuel effects on liquid-phase penetration in DI sprays, SAE Paper, No. 1999-01-0519, (1999).

[19] J. F. Ely and M. L. Huber, NIST Thermophysical Properties of Hydrocarbon Mixtures Database (SUPERTRAPP) Version 1.0 Users' Guide, National Institute of Standards and Technology, (1992).

[20] S. Ohe, Estimate Method of Property Constants for Beginner, *Nikkan Engineering Paper Corp.* (in Japanese) (1985) 215-221.

[21] C. Espey, J. E. Dec, T. A. Litzinger and D. A. Santavicca, Quantitative 2-D fuel vapor concentration imaging in a firing D.I. diesel engine using planar laser-induced rayleigh scattering, SAE Paper, No. 940682, (1994).

[22] C. Espey and J. E. Dec, The effect of TDC temperature and density on the liquid-phase fuel penetration in a D.I. diesel engine, SAE Paper, No. 952456, (1995).

[23] C. Espey, J. E. Dec, T. A. Litzinger and D. A. Santavicca, Planar laser rayleigh scattering for quantitative vapor-fuel Imaging in a diesel jet, *COMBUSTION AND FLAME, 109* (1997) 65-86.

[24] J. T. Hodges, T. A. Baritaud and T. A. Heinze, Planar liquid and gas fuel and droplet size visualization in a DI diesel engine, SAE Paper, No. 910726. (1991).

[25] T. A. Baritaud, T. A. Heinze and J. F. Le Coz, Spray and self-ignition visualization in a DI diesel engine, SAE Paper, No. 940681. (1994).

[26] J. Senda, T. Kanda, M. Al-Roub, P. V. Farrell, T. Fukami and H. Fujimoto, Modeling spray impingement considering fuel Film Formation on the Wall, SAE Paper, No. 970047, (1997).